AIP | Journal of Applied Physics

Influence of the metallic contact in extreme-ultraviolet and soft x-ray diamond based Schottky photodiodes

I. Ciancaglioni, C. Di Venanzio, Marco Marinelli, E. Milani, G. Prestopino et al.

Citation: J. Appl. Phys. **110**, 054513 (2011); doi: 10.1063/1.3633219
View online: http://dx.doi.org/10.1063/1.3633219
View Table of Contents: http://jap.aip.org/resource/1/JAPIAU/v110/i5
Published by the American Institute of Physics.

Influence of the metallic contact in extreme-ultraviolet and soft x-ray diamond based Schottky photodiodes

I. Ciancaglioni,[1] C. Di Venanzio,[1] Marco Marinelli,[1] E. Milani,[1] G. Prestopino,
[1]C. Verona,[1,a)] G. Verona-Rinati,[1] M. Angelone,[2] M. Pillon,[2] and N. Tartoni[3]
[1]*Dip. di Ing. Meccanica, Università di Roma "Tor Vergata," Roma 00133, Italy*
[2]*Associazione EURATOM-ENEA sulla Fusione, Frascati, Roma 00044, Italy*
[3]*Diamond Light Source, Harwell Science and Innovation Campus, Chilton-Didcot, OX11 0DE Oxfordshire, United Kingdom*

(Received 21 June 2011; accepted 2 August 2011; published online 15 September 2011)

X-ray and UV photovoltaic Schottky photodiodes based on single crystal diamond were recently developed at Rome "Tor Vergata" University laboratories. In this work, different rectifying metallic contact materials were thermally evaporated on the oxidized surface of intrinsic single crystal diamond grown by chemical vapor deposition. Their impact on the detection performance in the extreme UV and soft x-ray spectral regions was studied. The electrical characterization of the metal/diamond Schottky junctions was performed at room temperature by measuring the capacitance–voltage characteristics. The diamond photodiodes were then tested both over the extreme UV spectral region from 10 to 60 eV by using He-Ne DC gas discharge as a radiation source and toroidal vacuum monochromator, and in the soft x-ray range from 6 to 20 keV at the Diamond Light Source synchrotron x-ray beam-line in Harwell (UK). In both experimental setups, time response and spectral responsivity were analyzed for all the investigated Schottky contact materials. A good agreement between the experimental data and theoretical results from Monte Carlo simulations is found © *2011 American Institute of Physics*. [doi:10.1063/1.3633219]

I. INTRODUCTION

Diamond is a semiconducting material with extreme optical and electronic properties[1,2] that make it an ideal material for the fabrication of high performance visible-blind detectors for ultraviolet (UV) and soft x-ray (XR) radiation.[3] Several attempts were made to build up photodetectors from natural or synthetic diamonds.[4,5] A great effort is also being devoted to produce devices from synthetic single crystal diamond (SCD) films grown by homoepitaxial chemical vapor deposition (CVD) onto low-cost SCD substrates.[6,7]

Different photodetector structures based on CVD diamond have been reported by several research groups.[8,9] A promising approach is to use a Schottky photodiode (PD) in a multilayered transverse configuration due to its low leakage current, low noise level, zero-bias operation, no signal due to secondary electrons, fast response time, and good responsivity.[10,11] The main detection mechanism in Schottky photodiodes is based on collection of photogenerated electron–hole pairs in the depleted layer region beneath the Schottky metal contact so that the development of good Schottky contacts plays a significant role on the overall detection performance of such devices.

Many authors have studied the electrical properties of metal/diamond interfaces evidencing the importance of physico-chemical treatments of diamond surface and of Schottky metal contacts.[12,13] The aim of this paper is to perform a systematic analysis of several rectifying metallic contact materials on our diamond based photodiodes to investigate the physical properties of different metal/diamond interfaces and their role in the detection performance in the extreme UV and soft x-ray spectral region. To this purpose, electro-optical measurements such as *C-V* characteristics, spectral responsivity and time response evaluation were performed.

II. EXPERIMENTAL SETUP

The diamond photodetectors investigated in the present study consist of a multilayered structure obtained by a three step deposition process as reported in Ref. 11. This procedure allows a nominally intrinsic single crystal diamond layer, which is the detecting region, sandwiched between a Schottky metallic contact of 3 mm in diameter and a highly conductive boron doped diamond layer, acting as backing contact. In Ref. 11, it has been also shown that the nominally intrinsic layer acts as a slightly p-type doped layer with a concentration of acceptor of the order to 10^{14} cm^{-3}. The scheme of the device is shown in Fig. 1.

Due to the small penetration depth of the extreme UV radiation in diamond,[14] a 2 μm thick intrinsic diamond layer was used for the measurement in this spectral region (UV-PD in the following). In the case of soft x-ray detection, similar detectors with an intrinsic diamond thickness of about 30 μm were used instead (XR-PDs in the following) due to the higher penetration depth of the incident radiation.

UV-PDs were fabricated using Schottky contacts made of five different semitransparent metals on the very same SCD: 63 Å thick silver (Ag), 68 Å thick platinum (Pt), 100 Å thick aluminum (Al), 120 Å thick chromium (Cr), and 70 Å thick gold (Au). Their thickness was measured directly

a)Author to whom correspondence should be addressed. Electronic mail: claudio.verona@uniroma2.it.

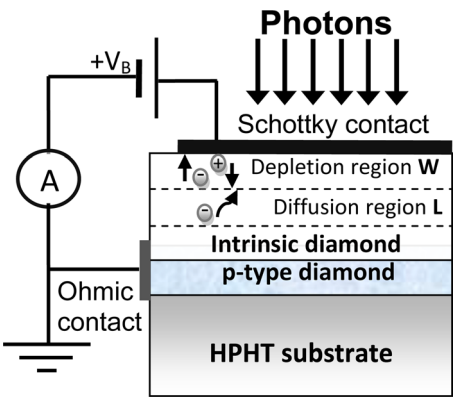

FIG. 1. (Color online) Schematic representation of Schottky diamond photodiodes.

by a thickness monitor with a resolution of about 1 Å. Experimental tests were performed according to the following procedure: (i) the intrinsic diamond surface of the UV-PD detector was metalized with a metallic contact, (ii) measurements were performed and, (iii) the diamond surface was carefully cleaned by wet etching before depositing a new contact. The whole procedure was repeated a few times for each metal contact to verify the repeatability and the reliability of the cleaning/deposition process. As reported in Ref. 15, for contacts in the nanometer thickness range, contact inhomogeneity may have an impact on the electrical properties. Although we cannot rule out such an effect in our case, scanning electron microscope (SEM) observation did not evidence any lack of uniformity.

The UV-PD has been tested in our laboratories over the extreme UV spectral region from 10 to 60 eV using a He-Ne DC gas discharge as a radiation source and a toroidal grating vacuum monochromator (Jobin Yvon model LHT-30) with a 5 Å wavelength resolution. The photodetector response was compared to that of a calibrated NIST silicon photodiode[16] placed in the same position by using a three dimension mechanical (X-Y-Z) stage powered by stepper motors. The photocurrent was measured by a Keithley 6517 A electrometer. The UV-PD was encapsulated in a copper/vetronite shielded housing with a 2 mm pinhole to collimate the radiation on the sensitive area of the detectors and to obtain the same illuminated area on the silicon photodiode. In such a housing, the top surface metal contact is grounded, and the photocurrent is measured from p-type diamond electrode so that the signal is not affected by secondary electron emission current from the illuminated contact.[17–19] Only the internal photocurrent produced inside the diamond is thus measured.

In the case of the x-ray detectors, four similar XR-PDs with different metallic contacts were tested at the beamline B16 of Diamond Light Source (DLS) synchrotron: 100 nm thick Al contact, 25 nm thick Pt contact, 22 nm thick Au contact, and 20 nm Cr thick contact. A monochromatic beam delivered by a double crystal monochromator was used in the region from 6 keV to 20 keV. The beam was focused by the beam line optics (spot size about 300 μm) so as to be completely intercepted by the sensitive area of the detector. Due to the low energy of the beam, a tube filled with helium was used to minimize the air path and to reduce the absorption. The detectors were operated in current mode and a variable gain low noise current amplifier FEMTO model DLPCA-200 (Ref. 20) was used as front-end electronics. The XR-PDs under test were placed in a grounded metal box on top of a high resolution translational stage so that high precision positioning of the detector with respect to the beam was achieved. The time response of the XR-PDs was measured by using a rotating mechanical chopper placed in front of the x-ray radiation beam and a Tektronix oscilloscope. Finally, a PTB calibrated silicon detector was also placed on the translational stage nearly the diamond detector and used during the energy response measurement.

III. RESULTS AND DISCUSSIONS

The *I-V* characteristics of the metal/diamond Schottky junction of the photodetector were performed at room temperature by using a Keithley 6517 A pico-ampere meter. The *I-V* characteristics were obtained by applying a voltage to the p-type diamond layer while earthing the metallic contact. Figure 2 shows the typical *I-V* characteristic of the diamond Schottky photodiode. A very high rectification ratio of order of 10^8 was observed at ± 3 V. In the inset of the figure, the *I-V* characteristic in forward region for the different metallic contacts is also reported. In this region, the forward current density is well described by the thermionic emission (TE) theory and a rough approximation of the Schottky barrier height, and the ideality factor can be extracted for the different metallizations. Ideality factors below 1.8 were estimated for all the investigated contacts with barrier heights in the range between 1.8 and 2 eV.

Capacitance-voltage (*C-V*) measurements were performed by using an Agilent 4284 A LCR meter to get information on the depletion region width of the Schottky barrier formed by the metal electrode, which extends within the intrinsic diamond layer. In first approximation, at low frequency, the junction capacitance of the device is approximated to that of a parallel plate capacitor so that the depletion thickness W of the detector as a function of the applied bias voltage V_B was estimated from the *C-V* data according to the following equation:[21]

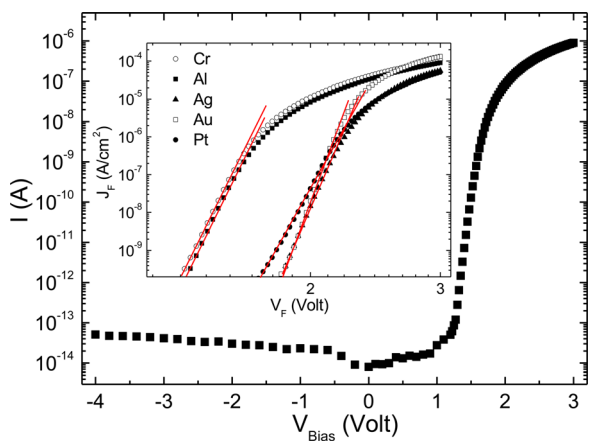

FIG. 2. (Color online) Current–voltage (*I-V*) characteristics. Inset: magnified view of *I-V* characteristic in forward voltage region for all the investigated metallic contacts.

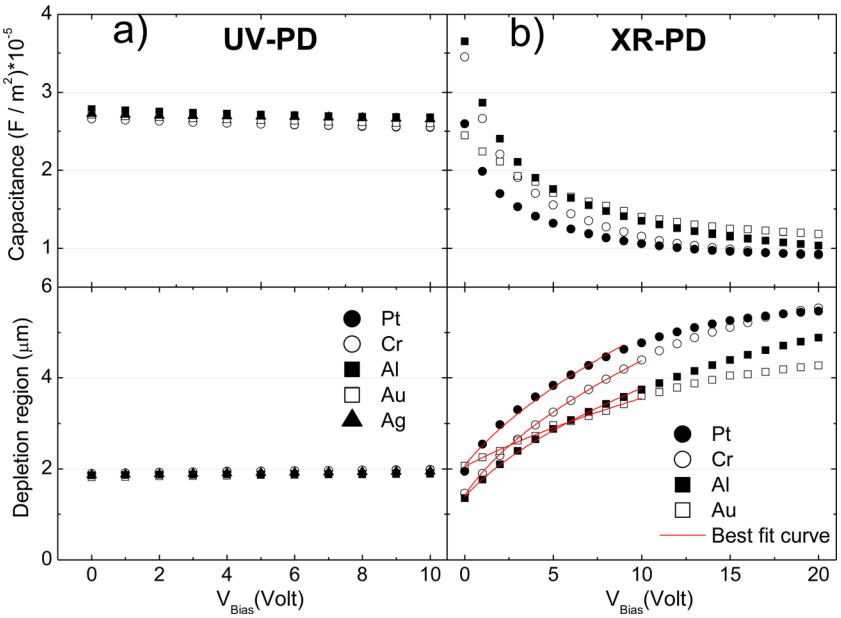

FIG. 3. (Color online) Capacitance–voltage (*C-V*) characteristics and corresponding depletion thickness (*W*) of (a) UV-PD and (b) XR-PD detectors, respectively. The full lines are the best fit calculated by Eq. (1).

$$W = \sqrt{\frac{2\varepsilon_0\varepsilon_r(V_B + V_{BI})}{qN_A}} = \varepsilon_0\varepsilon_r\frac{A}{C} \qquad (1)$$

where A is the contact area, q the electric charge, ϵ_o the dielectric constant of free space, ϵ_r the diamond dielectric constant, V_{BI} the built-in potential at the Schottky barrier, and N_A the concentration of electrically active defects.

Figure 3 shows the capacitance–voltage curves for both UV-PD and XR-PDs with different metallic contacts at room temperature and at 100 kHz frequency in the reverse bias region. Using Eq. (1), a depletion thickness of about 2 μm is extracted from the experimental data for the UV-PD detectors at all bias voltages applied (see Fig. 3(a)). Such a thickness is approximately the nominally intrinsic diamond film thickness thus demonstrating that the sensing layer is fully depleted.

For the XR-PDs (see Fig. 3(b)), the width of the depletion layer at zero bias voltage is evaluated to be approximately 1.25 μm, 1.4 μm, 2 μm, and 2.15 μm for Al, Cr, Pt, and Au contacts, respectively. In this case, the depletion width increases extending into the thick intrinsic diamond layer as reverse bias increases up to 20 V.

Both the active defects concentration N_A and the built-in potential V_{BI} can be derived from the results reported in Fig. 3(b) for the XR-PDs. The best fit of the experimental data was performed by using Eq. (1) in the low voltage region, the results of which are summarized in Table I. For the four tested XR-PDs devices, N_A is of the order of 10^{14} cm^{-3}.

In the next sections, the effect of the metallic contact materials on time response and responsivity of both diamond based photodetectors is analyzed.

TABLE I. Fit parameters of Eq. (1).

Detector	Active defects concentration N_A (cm^{-3})	Built-in potential V_{BI} (*V*)
XR-PD_Al	5.0×10^{14}	1.5
XR-PD_Cr	3.6×10^{14}	1.2
XR-PD_Pt	3.1×10^{14}	2.1
XR-PD_Au	7.3×10^{14}	4.8

A. Extreme UV characterization

The normalized time response under illumination of He-Ne DC gas discharge at zero applied voltage is reported in Fig. 4 for the UV-PD with different metal contacts. The UV-PD metalized with Ag, Pt, Al, and Cr shows fast rise and decay times of the photocurrent. The responses are reproducible, and undesired effects such as persistent photocurrent and priming or memory effects are negligible. The response time, which was estimated to be about 60 ms, is completely ascribed to the electrometer preamplifier time constant. On the other hand, the detector operating with Au contact clearly shows a slow component of the photocurrent to reach the

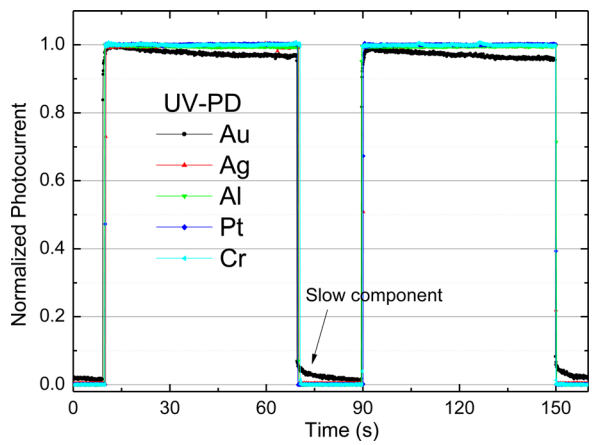

FIG. 4. (Color online) Normalized time response under illumination of He–Ne DC gas discharge radiation source of the UV-PD for the different metals.

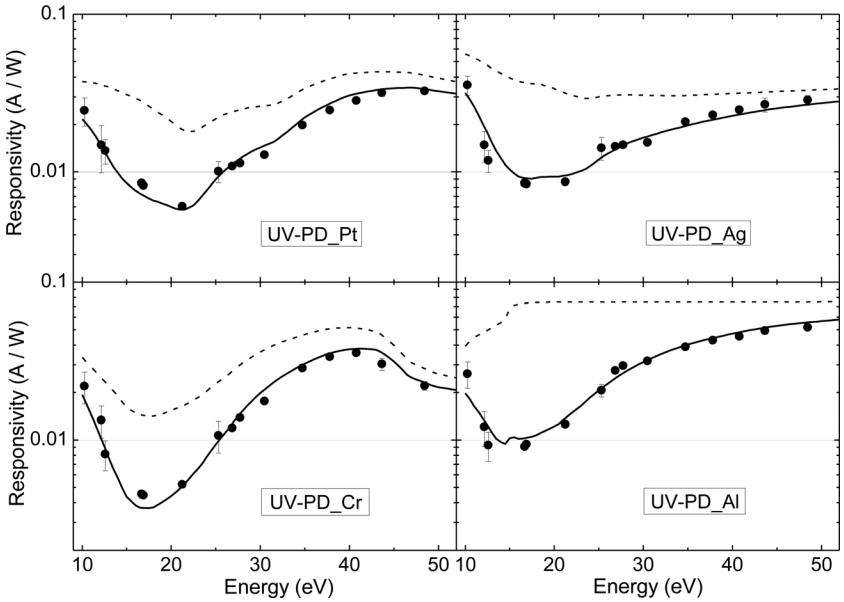

FIG. 5. Absolute spectral responsivity of UV-PD between 10 and 60 eV for each different metallic contact. The dashed lines are the results of the fit calculated by Eq. (2). The solid line curves correspond to Eq. (2) multiplied by the exponential term related to the dead diamond layer.

plateau value once irradiated and a photocurrent persistence decaying exponentially with a time constant of about 4 s. This behavior of the Au contact has been checked by repeating a few times the whole cleaning/metallization/test procedure, both on the investigated SCD sample and on different samples. In all cases, a slow component of the photocurrent was always observed using thermally evaporated Au.

The emission spectrum of the DC discharge He-Ne lamp in the 10-60 eV energy range was then measured by the UV-PD for each different metallic contact. The absolute responsivity of UV-PD, expressed in amperes per watt (A/W), was evaluated from the obtained spectra by comparing the diamond response with the one of a calibrated silicon photodiode. The results are shown in Fig. 5. All the obtained responsivity curves show a minimum between 15 and 20 eV. A monotonically increasing responsivity is observed at higher photon energy for all cases with the exception of Cr, the responsivity of which decreases above 40 eV.

An accurate estimation of the responsivity obtained from the Au contact is not reported in this paper because the photoresponse was affected by persistent photocurrent and high noise even at low level signals.

The experimental data were compared with the theoretical curve obtained by calculating the fraction of energy deposited in the diamond layer and by taking into account absorption losses in the Schottky metal electrode:[22]

$$R(A/W) = \frac{(1 - e^{-\alpha_{\mathrm{diam}} D_{\mathrm{diam}}}) e^{-\alpha_{\mathrm{Metal}} d_{\mathrm{Metal}}}}{E(eV)} \qquad (2)$$

where E is the mean electron-hole pair creation energy (13.2 eV for diamond), α is the absorption coefficient of the materials, D_{diam} is the active diamond thickness, and d_{Metal} is the thickness of the metallic contact. The transmission values in Eq. (2) are readily calculated from the material thickness and the known x-ray optical data for elements.[23] The dashed lines plotted in Fig. 5 are the results of the fit calculated according to Eq. (2). The thickness of the tested metallic contacts and the effective thickness of intrinsic diamond estimated by the *C-V* curves were taken into account. Clearly, the fit curves do not reproduce the experimental data, thus indicating that other contributions must be considered when calculating the device responsivity. Because the UV-induced charges are generated at the metal/diamond interface, such a contribution could be related to the diamond surface properties. In the investigated photon energies, the penetration depth of photons in diamond shows a deep minimum at about 16 eV,[14,23] the trend of which is qualitatively similar to the responsivity curves observed in Fig. 5. This suggests the existence of a dead layer located at diamond surface probably related to the recombination of photogenerated carriers close to the metal-diamond interface.[24,25] In this region, in fact, the photogenerated carriers could be trapped very efficiently by the defects of the diamond surface giving a low contribution to the photocurrent. Under this assumption, in first approximation, Eq. (2) must be multiplied by the additional term $\exp(-\alpha_{\mathrm{diam}} d_{\mathrm{diam}})$, where $\alpha_{\mathrm{diam}}(\lambda)$ is the diamond absorption coefficient and d_{diam} is the thickness of the dead diamond layer.

The responsivity curves reported in Fig. 5 as solid lines are the results of the fits using the values reported in Table II. They show a good agreement with the experimental data for all tested metallic contacts.

B. Soft x-ray characterization

Figure 6 shows the XR-PD photocurrent measured during 10 keV x-ray irradiation chopped at 3.9 kHz. Rise and

TABLE II. Fit parameters of Eq. (2) multiplied by the additional term exp $(-\alpha_{\mathrm{diam}} d_{\mathrm{diam}})$.

Detector	Depletion layer W (μm) = D_{diam}	Dead diamond layer d_{diam} (nm)	Metal contact thickness d_{metal} (nm)
UV-PD_Al	1.84	7.0	10
UV-PD_Cr	1.90	5.5	12
UV-PD_Pt	1.91	5.5	6.8
UV-PD_Ag	1.86	5.8	6.3

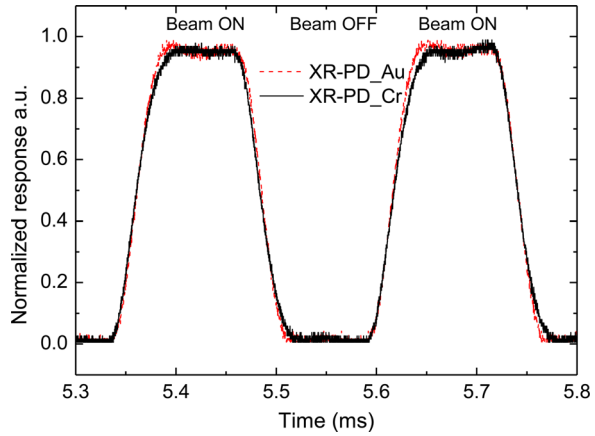

FIG. 6. (Color online) Temporal response of the XR-PDs under 10 keV x-ray beam chopped at 3.9 kHz.

decay times of the photoresponse of about 50 μs are observed for all the investigated contact metals, a value roughly corresponding to the full opening time of the aperture of the mechanical chopper. The slow component observed in the UV measurement when using gold contact, could not be measured in this case, being its time scale approximately five orders of magnitude longer than the adopted chopping time.

The absolute responsivities versus x-ray photon energy were obtained by comparing the currents measured in diamond with the PTB silicon current and applying the proper calibration factors. The experimental data reported in Fig. 7 were obtained for the tested XR-PDs in the 6 keV to 20 keV energy range. Due to its 30 μm thickness, the intrinsic diamond layer is only partially depleted in the adopted unbiased operating conditions and carriers generated outside the depletion region within the minority carrier diffusion length L are collected too (see Fig. 1). Therefore both drift and diffusion contribution to the current due to photogenerated carriers must be taken into account. Previous results[11,26] show that the diffusion length L is about 2.6 μm. This value is added to the depletion layer thickness calculated from the C-V curves to evaluate the effective thickness of the active diamond layer of XR-PDs.

The energy deposited in the diamond was thus obtained by using the actual thickness values reported in Table III for both the evaporated metal contact and the active diamond layer.

The x-ray high penetration depth makes the previously mentioned dead diamond layer negligible. The fitting curves (dashed lines in Fig. 7), however, do not satisfactorily reproduce the experimental the data, especially for Pt and Au contacts. The described procedure only takes into account energy deposited in the detector by carrier photo-generation.

Energy deposition is, however, an inherently stochastic process in which other channels besides carrier photogeneration occur, each with its proper cross section and detector geometry dependence. In particular, in the x-ray region, it is very important to take into account the physical interactions of radiation with matter, i.e., Compton photon scattering, photo and knock-on secondary electrons, which are not considered in the fitting procedure described in the preceding text. To accurately simulate the ionizing mechanism inside a detector volume, Monte Carlo methods must therefore be used. A 3-D Monte Carlo simulation of the experimental data was performed by using the MCNP-5 radiation transport code.[27] The simulation was carried out using the data reported in Table III. The results of the Monte Carlo simulation, reported in Fig. 7 as solid lines, are now in good agreement with the experimental data.

The observed large difference in responsivities among the four tested XR-PDs reflects the difference interaction between x-ray beam and different metal contacts material. In particular, the responsivity of detectors with Pt and Au contact is higher than that of detectors using Al and Cr contacts. Indeed, platinum and gold have an atomic number ($Z_{Pt} = 78$ and Z_{Au} =79) higher than aluminum and chromium ($Z_{Al} = 13$ and $Z_{Cr} = 24$), so as to produce many photo and knock-on secondary electrons that substantially contribute to the energy deposition in the diamond layer. This is even more evident at high photon energies, above 10 keV, where a clear

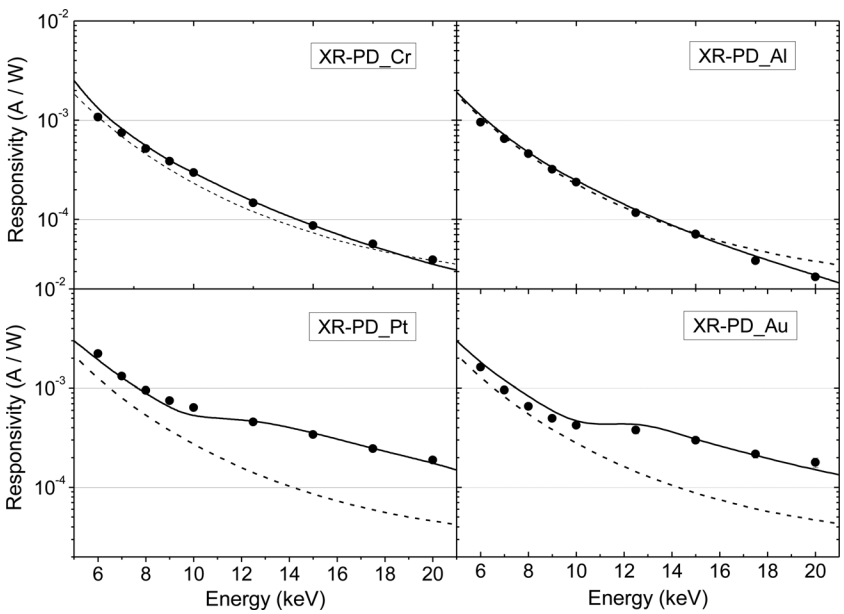

FIG. 7. Experimental and theoretical spectral responsivity of the XR-PDs in the range from 6 to 20 keV. The dashed lines are the results of the fit calculated by Eq. (2). The solid line curves correspond to Monte Carlo simulations.

TABLE III. Parameters employed in the Monte Carlo simulations.

Detector	Depletion layer W (μm)	Diffusion length L (μm)	Active diamond thickness $W+L$ (μm) $=D_{\text{diam}}$	Metal contact thickness d_{metal} (nm)
XR-PD_Al	1.25	2.60	3.85	100
XR-PD_Cr	1.40	2.60	4.00	20
XR-PD_Pt	2.00	2.60	4.60	25
XR-PD_Au	2.20	2.60	4.80	22

change in the behavior of the responsivity curves is observed for both metals.

IV. CONCLUSIONS

Performance parameters such as time response and spectral responsivity were analyzed for a single crystal diamond photodiode in the extreme UV and soft x-ray spectral region as a function of the Schottky metal contact material. The results show that the electro-optical performance of a diamond detector is influenced by the used metal and the energy dependent absorption length of the detected radiation.

In the extreme UV region, all contacts, except the Au contact, show similar behavior in terms of time response, and no undesired effects such as persistent photocurrent or memory effects are observed. The responsivity of UV-PD with Ag, Al, Cr, and Pt contacts show similar trends in the energy range from 10 eV up to 60 eV, increasing toward the edges of the investigated spectral range and showing a minimum at intermediate photon energies between 15 and 20 eV. This is attributed to the photon induced carriers, which, in this spectral region, are generated mainly close to the metal/diamond interface. The results of the fitting procedure show that a dead diamond layer must be taken into account; this is most likely related to the high recombination of photo-generated carriers near the metal electrode and significantly affects the detector responsivity. The thickness of this dead layer region was observed in the range between 5.5 and 7 nm.

The spectral responsivities of the XR-PDs were measured in the range from 6 to 20 keV, showing a different trend as a function of the metallic contacts. The experimental data were compared with the results of a 3 D Monte Carlo photon and electron transport calculation. A good agreement between experimental data and simulated curves was obtained, and the main features of the responsivity curves were explained in terms of the different Z-numbers of the metals used for the contacts.

[1]J. E. Field, *Properties of Diamond* Academic, London, 1979.
[2]J. Prins, *The Physics of Diamond*, edited by A. Paoletti and A. Tucciarone (IOS Press, Amsterdam, 1997).
[3]J.-F. Hochedez, J. Alvarez, F. D. Auret, P. Bergonzo, M.-C. Castex, A. Deneuville, J. M. Defise, B. Fleck, P. Gibart, S. A. Goodman, O. Hainaut, J.-P. Kleider, P. Lemaire, J. Manca, E. Monroy, E. Munoz, P. Muret, M. Nesladek, F. Omnes, E. Pace, J. L. Pau, V. Ralchenko, J. Roggen, U. Schuhle, and C. Van Hoof, Diamond Relat. Mater. **11**, 427 (2002).
[4]L. Barberini, S. Cadeddu, and M. Caria, Nucl. Instrum. Methods Phys. Res. A, **460**, 127 (2001).
[5]R. D. McKeag and R. B. Jackman, Diamond Relat. Mater. **7**, 513 (1998).
[6]T. Teraji, S. Yoshizaki, H. Wada, M. Hamada, and T. Ito, Diamond Relat. Mater. **13**, 858 (2004).
[7]J. H. Kaneko, T. Teraji, Y. Hirai, M. Shiraishi, S. Kawamura, S. Yoshizaki, T. Ito, K. Ochiai, T. Nishitani, and T. Sawamura, Rev. Sci. Instrum. **75**, 358 (2004).
[8]Meiyong Liao, Y. Koide, and J. Alvarez, Appl. Phys. Lett. **88**, 33504 (2006).
[9]A. BenMoussa, K. Haenen, U. Kroth, V. Mortet, H. A. Barkad, D. Bolsee, C. Hermans, M. Richter, J. C. De Jaeger, and J. F. Hochedez, Semicond. Sci. Technol. **23**, 035026 (2008).
[10]M. Angelone, M. Pillon, M. Marinelli, E. Milani, G. Prestopino, C. Verona, G. Verona-Rinati, I. Coffey, A. Murari, and N. Tartoni, Nucl. Instrum. Methods Phys. Res. A **623**, 726 (2010).
[11]S. Almaviva, M. Marinelli, E. Milani, G. Prestopino, A. Tucciarone, C. Verona, G. Verona-Rinati, M. Angelone, M. Pillon, I. Dolbnya, K. Sawhney, and N. Tartoni, J. Appl. Phys. **107**, 1 (2010).
[12]R. D. Mckeag, R. D. Marshall, B. Baral, S. S. M. Chan, and R. B. Jackman, Diam. Relat. Mater. **6**, 374 (1997).
[13]C. Jany, F. Foulon, P. Bergonzo, and R. D. Marshall, Diam. Relat. Mater. **7**, 951 (1998).
[14]D. Palik, *Handbook of Optical Constants of Solids II* Academic, New York, 1991.
[15]J. Alvarez, F. Houzé, J. P. Kleider, M. Y. Liao, and Y. Koide, Superlattices Microstruct. **40**, 343 (2006).
[16]See http://www.ird-inc.com for information about international radiation detectors (IRDs).
[17]M. C. Rossi, Spaziani, F. Conte, and G. Ralchenko V., Diam. Relat. Mat. **14**, 552 (2005).
[18]T. Saito and K. Hayashi, Appl. Phys. Lett. **86**, 122113 (2005).
[19]I. Ciancaglioni, M. Marinelli, E. Milani, G. Prestopino, C. Verona, G. Verona-Rinati, M. Angelone, and M. Pillon, J. Appl. Phys. **110**, 014501 (2011).
[20]See www.femto de for more information on the low noise current amplifier FEMTO.
[21]D. Neamen, *Semiconductor Physics and Devices: Basic Principles* (McGraw-Hill Companies, Chicago 1997).
[22]S. M. Sze, *Physics of Semiconductor Devices* (Wiley, New York, 1981).
[23]http://henke. lbl.gov/optical_constants/filter2.forhtml for information on filter transmission.
[24]J. W. Keister and J. Smedley, Nucl. Instrum. Methods Phys. Res. A **606**, 774 (2009).
[25]S. Almaviva, M. Marinelli, E. bMilani, G. Prestopino, A. Tucciarone, C. Verona, G. Verona-Rinati, M. Angelone, and M. Pillon, Diam. Rel. Mater. **19**, 78 (2010).
[26]A. Lo Giudice, P. Olivero, C. Manfredotti, M. Marinelli, E. Milani, F. Picollo, G. Prestopino, A. Re, V. Rigato, C. Verona, G. Verona-Rinati, and E. Vittone, Phys. Status Solidi (RRL) **5**, 80 (2011).
[27]See http://mcnp-green.lanl.gov/ for information about MCNP-5 radiation transport code.